VTT Technical Research Centre of Finland

Stochastic model-predictive control of district-scale building energy systems using SpineOpt

Rasku, Topi; Hasan, Ala

Published in:
Proceedings of Building Simulation 2023

Accepted/In press: 28/09/2023

Document Version
Peer reviewed version

Stochastic model-predictive control of district-scale building energy systems using SpineOpt

Topi Rasku[1], Ala Hasan[1]
[1]VTT Technical Research Centre of Finland Ltd, Espoo, Finland

Abstract

Model predictive control of buildings is a vibrant field, but mostly focuses on buildings as "price-takers". While simplified resistance-capacitance building models have previously been employed within large-scale energy system frameworks to analyse market impacts, tools for stochastic programming are scarce. In this work, we demonstrate the viability of the SpineOpt energy system modelling framework for stochastic model predictive control of an imaginary six-building district using different weather and price forecasts, achieving reasonable performance and cost savings comparable with existing literature. The used methods could be scaled up to city or nation-scale energy system studies, or be utilised for electricity market bidding of aggregated building flexibility.

Highlights

- SpineOpt demonstrated capable of stochastic model predictive control of district-scale energy systems.
- Stochastic programming beyond district-level has potential applications for electricity market bidding of aggregated building flexibility.
- Uncertainty about weather conditions and electric load had surprisingly little impact on the district operations.

Introduction

Electrification of traditionally fossil-fuelled sectors like heating and transportation holds a lot of promise for decarbonising our economies. However, supplying the resulting electricity demand with variable renewable electricity requires significant flexibility from the demand side. Since buildings contain considerable inherent thermal inertia, their heating, ventilation, and air conditioning (HVAC) as well as domestic hot water (DHW) systems can be harnessed for demand-side management (DSM). Thus, heating sector electrification can help mitigate its impacts on the power system, although accessing this building-level energy flexibility requires sophisticated control systems, e.g. model predictive control (MPC).

Drgoňa et al. (2020) present an excellent review into the breadth of literature on MPC of building systems. Common objectives include minimising energy consumption, cost, or CO_2 emissions, while maintaining thermal comfort, achieving savings around 10–60 % depending on the case study as reviewed by Taheri et al. (2022). However, while these studies only consider buildings as "price-takers", in reality, electricity markets would adapt when faced by widespread DSM. Thus, in order to study energy market scale impacts or viability of widespread building energy flexibility, it needs to be depicted within large scale energy system models. Bloess et al. (2018) provide a great review on the topic of previous power-to-heat studies on energy system scales, some including residential building energy flexibility as well. Ever since Hedegaard and Balyk (2013) pioneered the use of simplified resistance-capacitance (RC) building models for studying flexible residential heat pump investments for wind power integration, similar approaches have been successfully employed by e.g. Cooper et al. (2016) for examining impacts of mass adoption of heat pumps on peak load in the UK, by Arteconi et al. (2016) and Rasku and Kiviluoma (2018) for looking into the impact of HVAC DSM market penetration in Belgium and Finland respectively, as well as by Huckebrink and Bertsch (2022) comparing different flexible heating options for Germany. Recently, deterministic MPC for individual buildings has been demonstrated using the Backbone energy system modelling framework by Rasku et al. (2023).

To the authors' best knowledge, simplified RC thermal models of building energy flexibility for energy system scale studies have not been previously examined under price, weather, and load uncertainty. In this work, we demonstrate the open source energy system modelling framework SpineOpt for stochastic MPC of a small imaginary district capable of utilising the building-level energy flexibility. This enables studying the impact of widespread building energy flexibility on energy system operations while accounting for uncertainty. Furthermore, similar approaches could be used for electricity market bid optimisation for aggregated building energy flexibility.

Methods

In this work, we demonstrate that district-scale stochastic MPC can be implemented and solved using the SpineOpt energy system modelling framework by Ihlemann et al. (2022). In brief, the mixed-integer-linear-programming-based SpineOpt is primarily designed for solving large-scale energy system investment planning, unit commitment, and economic dispatch problems. However, thanks to its generic system and temporal depictions, it can be adapted to represent systems with drastically different features. Since unit commitment and economic dispatch for large-scale energy systems are typically solved as rolling horizon optimisation problems as well, implementing simple MPC was achieved through model definitions and data alone, without the need to modify SpineOpt itself.

As a case study, a small electrically heated imaginary district of six different buildings with photovoltaic (PV) generation and a shared battery was set up. Simplified RC thermal models of the buildings were employed for capturing the flexibility in their heating and cooling demand. It is important to note that the district modelled in this work does not aim to be strictly realistic, but instead allow for easy examination of the MPC operation in order to verify SpineOpt performing in a reasonable manner. The Spine Toolbox (Kiviluoma et al. (2022)) workflow containing all the data and code used in this work has been made available by Rasku (2023) for interested readers.

The modelled district energy system

The modelled imaginary district contains six buildings, illustrated in Figure 1, based on the set of example buildings from IDA ESBO v1.13 (EQUA Simulation AB and Aalto University (2013)) adhering to the 2012 Finnish building regulations. For the sake of brevity, their detailed properties are not replicated here, and interested readers are instead referred to Rasku et al. (2023). The simplified RC building models, as well as their heating systems, were processed for SpineOpt using *ArchetypeBuildingModel.jl* (Rasku (2022)), with the district energy system illustrated in Figure 2 along with the building RC model. Note that even though the structure of the building RC models was identical, their properties were processed differently, as detailed in Rasku et al. (2023).

The building energy flexibility in the modelled district arises from the permitted indoor air and DHW tank temperature ranges presented in Table 1. While technically abiding by the Finnish building code by the Finnish Ministry of the Environment (2017), large rapid changes in the indoor air temperature are detrimental to the thermal comfort of the inhabitants. Ideally, proper indicators would be used to constrain the space heating flexibility, but implementing them within SpineOpt was outside the scope of this work.

Table 1: Permitted temperature ranges in the model.

Indoor air	Range
Detached house 1 (DH1)	21–25°C
Detached house 2 (DH2)	21–25°C
Apartment block (AB)	21–25°C
Office building (OB)	21–25°C
Service building (SB)	18–25°C
Communal building (CB)	21–25°C
DHW tanks	60–90°C

The buildings were assumed to be equipped with ground-to-water heat pump (G2WHP) systems for both space and water heating, as well as ground source cooling. For simplicity, the G2WHP was modelled using a seasonal performance factor (SPF) of 2.5 for space heating, corresponding to typical Finnish hydronic radiator heat distribution systems with 60 °C maximum temperature as suggested by the Finnish building code calculation guide by Eskola et al. (2012). For water heating using the G2WHP, an SPF of 1.58 was assumed accounting for direct electric topping up to 90 °C from the permitted minimum DHW tank temperature of 60 °C, while the ground source cooling used a SPF of 30 again based on Eskola et al. (2012). The DHW storage tanks for each building were sized to cover an assumed daily consumption of 1.64 litres per m^2, with their properties based on a Finnish building code calculation guide by Kurnitski et al. (2011). The resulting DHW tanks are frankly unrealistically large for the modelled non-residential buildings, but add more flexibility to the heating demand for this demonstration.

All of the modelled buildings were connected behind a common point of electricity import/export, which also included a shared 500 kW/1 MWh battery sized to cover the average appliance and lighting load of the district for roughly ten hours with a peak power five times the average load. The district also contained around 680 kWp of PV generation, distributed among the buildings to match their yearly total appliance and lighting loads. The import/export power was constrained to 1 MW, limiting excessive power peaks in the winter for the MPCs.

Processing data and forecasts

In order to perform stochastic MPC for the modelled district, forecasts were generated for the future electricity price, ambient temperature, solar irradiation, as well as appliance and lighting electric load of each building. For processing the PV generation as well as the ambient temperature and solar gains for the RC models, ERA5 (Hersbach et al. (2020)) weather data for the coordinates of the Helsinki-Vantaa airport for the years 2015–2022 was fetched via PyPSA/atlite (Hofmann et al. (2021)). Similarly, day-ahead electricity spot prices for the years 2015–2022 were obtained from the ENTSO-E transparency platform for

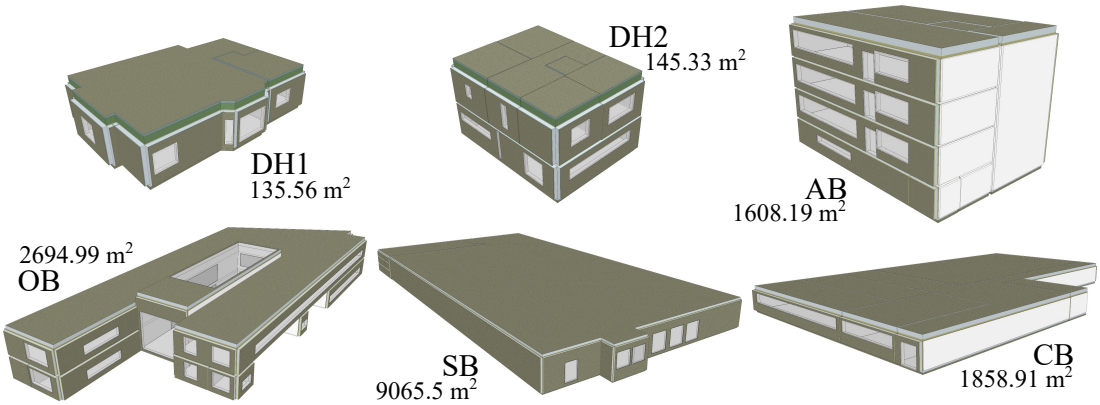

Figure 1: Illustrations of the modelled buildings and their gross floor areas (edited from Rasku et al. (2023)), including two detached houses (DH1 & DH2), an apartment block (AB), an office building (OB), a service building (SB), and a communal building (CB).

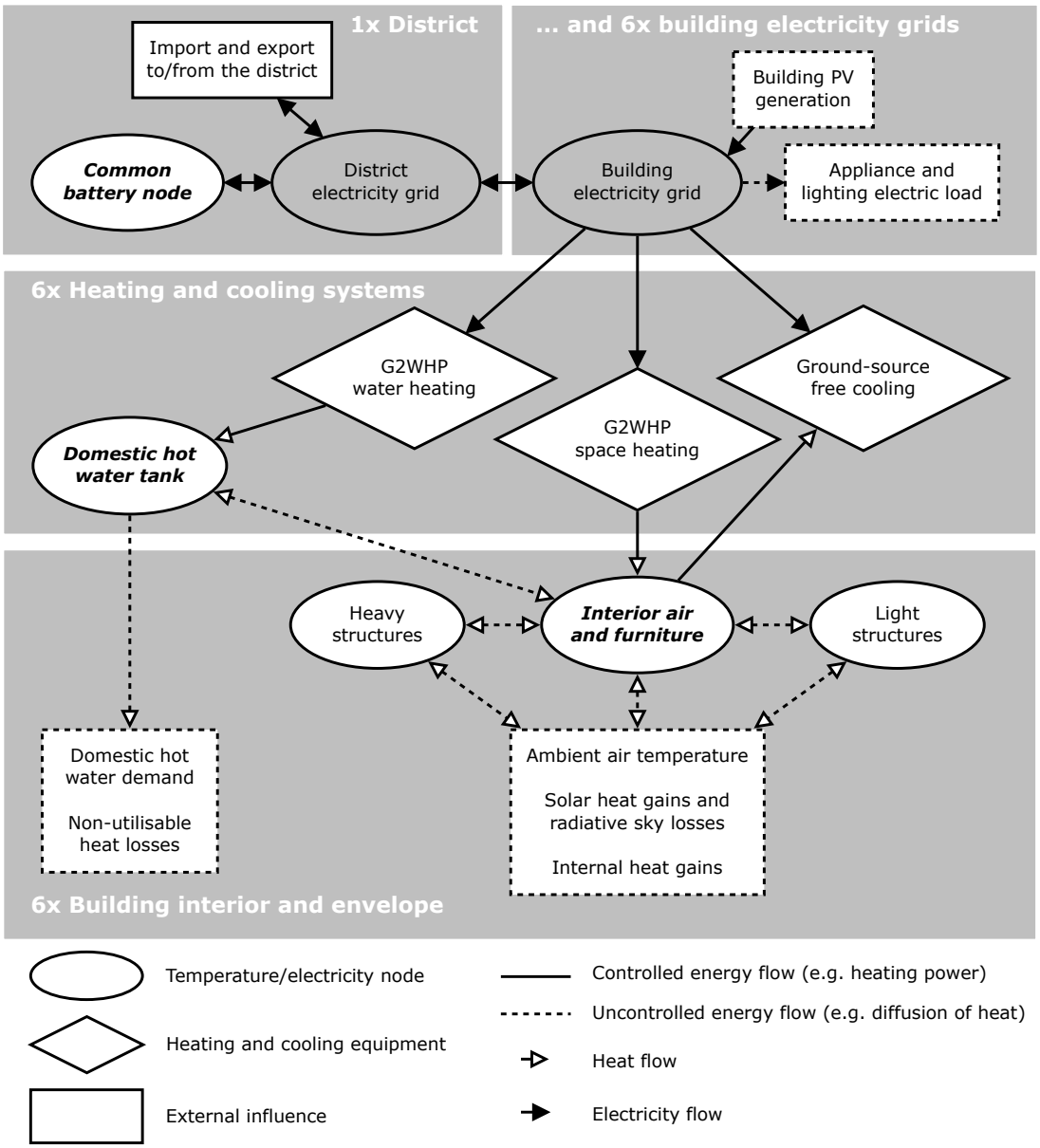

Figure 2: District model structure. Each building had their own "Building electricity grid" node, "Appliance and lighting electric load", heating systems, and RC models connected to the shared "District electricity grid" node.

Finland. A 10 % retail profit margin as well as electricity taxes and transmission fees totalling around 50 EUR/MWh were assumed to apply on top of the electricity import spot market price, while electricity exported from the district was sold at the spot price.

The appliance and lighting electric load profiles were based on the *Electricity Hourly Dataset* by Godahewa et al. (2020), containing 321 time series from 2012 to 2014. Inconsistent and season-dependent profiles were filtered out to improve the forecasts and avoid exaggerating the electric heating load. Six profiles that were deemed appropriate were hand-picked for the buildings, while the rest were used for generating the forecasts.

All of the aforementioned data was organised into four scenarios for the MPCs:

Realization contains data of what actually happens during the year 2022.

Mean represents the expected future, formed by taking the mean value for each hour of each sampled year.

Optimistic represents a best-case future, formed by taking the maximum ambient temperature and solar irradiation, as well as the minimum electricity price and load for each hour of each sampled year.

Pessimistic represents a worst-case future, formed similar to the above, but with opposite extremes.

When generating the scenarios, all time series data was first normalised for the processing using the mean value of each year, and later scaled for the year 2022 using its respective yearly mean values. 48-hour forecasts updating every 6 hours were then generated for SpineOpt, with the forecasts improved for the immediate future using via interpolation using the *Realization* data. However, note that the electricity day-ahead market was assumed to follow NordPool conventions, clearing the market and setting the prices for the next day at 12:00 UTC+00. Thus, the electricity prices were known 12–36 hours in advance for all scenarios depending on when the forecasts were created.

Unfortunately, due to lack of meaningful data, forecasts for DHW demand and internal heat gains could not be generated, and standard daily profiles from the Finnish building code calculation guide by Kurnitski et al. (2011) were used for every building and forecast. It is worth noting that forecasts generated this way are not particularly accurate or realistic. However, for the purposes of demonstrating the viability of stochastic MPC using SpineOpt in this work, they were deemed sufficient.

MPC using SpineOpt

Exploiting the generic design of SpineOpt, the rolling horizon optimal MPC problem for the district was implemented as

$$\begin{aligned}
\underset{\boldsymbol{v}}{\text{Min.}} \quad & f = \sum_{t\in\mathbb{T}} \sum_{s\in\mathbb{S}_t} p_s^{\text{weight}} \Delta_t \Big(&& (1)\\
& \quad p_{import,t,s}^{\text{vom_cost}} v_{import,into,district,t,s}^{\text{flow}} \\
& \quad - p_{export,t,s}^{\text{vom_cost}} v_{export,from,district,t,s}^{\text{flow}} \Big) \\
\text{s.t.} \quad & \frac{p_n^{\text{state_coeff}}}{\Delta_t} (v_{n,t,s}^{\text{state}} - v_{n,t-\Delta_t,s'}^{\text{state}}) && (2)\\
& = \sum_{n'\in\mathbb{N}_n} p_{n,n'}^{\text{diff_coeff}} \left(v_{n',t,s}^{\text{state}} - v_{n,t,s}^{\text{state}}\right) \\
& \quad - p_n^{\text{frac_state_loss}} v_{n,t,s}^{\text{state}} - p_{n,t,s}^{\text{demand}} \\
& \quad + \sum_{u\in\mathbb{U}_{into,n}} v_{u,into,n,t,s}^{\text{flow}} \\
& \quad - \sum_{u'\in\mathbb{U}_{from,n}} v_{u',from,n,t,s}^{\text{flow}} \\
& \quad \forall\, n\in\mathbb{N}, t\in\mathbb{T}, (s,s')\in(\mathbb{S}_t, \mathbb{S}_{t-\Delta_t}) \\
& v_{u,d,n,t,s}^{\text{flow}} = p_{u,d,n,d',n'}^{\text{ratio}} v_{u,d',n',t,s}^{\text{flow}} && (3)\\
& \quad \exists\,(u,d,n,d',n')\, p_{u,d,n,d',n'}^{\text{ratio}} \neq 0, \\
& \quad\quad \forall\, t\in\mathbb{T}, s\in\mathbb{S}_t \\
\text{and} \quad & p_n^{\text{state_min}} \le v_{n,t,s}^{\text{state}} \le p_n^{\text{state_cap}} && (4)\\
& \quad \exists\, n\, v_{n,t,s}^{\text{state}}, \forall\, t\in\mathbb{T}, s\in\mathbb{S}_t \\
& 0 \le v_{u,d,n,t,s}^{\text{flow}} \le p_{u,d,n,t,s}^{\text{capacity}} && (5)\\
& \quad \exists\,(u,d,n)\, p_{u,d,n,t,s}^{\text{capacity}}, \\
& \quad\quad \forall\, t\in\mathbb{T}, s\in\mathbb{S}_t
\end{aligned}$$

where p and v represent the used parameters and decision variables from SpineOpt respectively, with their names indicated by the superscripts and their indices by the subscripts. The set of time steps $t \in \mathbb{T}$ contains the hourly ($\Delta_t = 1\,\text{h}\,\forall\, t \in \mathbb{T}$) time steps for the current 48-hour optimisation horizon, while the set of scenarios $s \in \mathbb{S}_t$ contains the scenarios s active on each time step t. Meanwhile, the sets $n \in \mathbb{N}$, $u \in \mathbb{U}$, and $d \in \mathbb{D}$ represent the different nodes n, units u, and energy *flow* variable directions d of the modelled system illustrated in Figure 2. Please note that Eqs. (1)–(5) have been considerably simplified from their full formulation in SpineOpt, omitting a lot of unused features, as well as condensing some of the parameter and variable names.

The objective function in Eq. (1) captures the expected total costs of the district over the 48-hour optimisation horizon $t \in \mathbb{T}$ across the scenarios $s \in \mathbb{S}_t$ active on each time step. The *vom_cost* [€/Wh] parameters of the *import* and *export* units represent the hourly costs/profits of their respective *flow* [W] variables *into* and *from* the *district* electricity node. Each scenario s was assigned a probability *weight* to account for the expected costs across potentially mul-

tiple scenarios. Note that any potential costs of cycling the battery or the heating/cooling equipment were omitted for simplicity.

The node energy balance constraint in Eq. (2) enforces the key dynamics of the MPC. The *state_coeff* parameters represent the effective thermal masses [Wh/K] of the building RC model temperature nodes, while the *state* variables depict their temperatures [K]. The s and s' scenarios differ only over the boundary between the first and second time steps, when the model transitions from known *Realization* scenario to the future forecast scenarios for the rest of the horizon. The set $\mathbb{N}_n$ contains the nodes n' linked to the current node n via heat transfer coefficients [W/K], implemented using the *diff_coeff* parameter. Unfortunately, SpineOpt lacks dedicated parameters for ambient temperatures, but the related heat transfer term was separated into its node temperature and ambient temperature dependent constituents and implemented using a combination of the *frac_state_loss* [W/K] and *demand* [W] parameters. Similarly, the impact of solar and internal heat gains as well as DHW demand were processed into the *demand* parameter for the applicable nodes. For further details about the building RC model processing for SpineOpt, please refer to the *ArchetypeBuildingModel.jl* online documentation by Rasku (2022). The heating/cooling equipment *flow* variables add or remove heat from the temperature nodes while consuming electricity from the electricity nodes. Similarly, the *flow* variables handle electricity transfer between the *district* electricity node and the individual building electricity nodes. For the electricity nodes, the *state* variables were disabled, effectively reducing Eq. (2) to a power balance constraint instead.

The flow ratio constraint in Eq. (3) enforces the SPF between the *flow* variables *from* the input node n' *into* the output node n of each unit u, with the exception of the ground-source cooling units. Instead, the *ratio* parameter for the cooling units constrains the *flows from* both the building electricity node and the interior air and furniture node. Electricity transfer between the *district* electricity node and the building electricity nodes was assumed to have negligible losses.

Finally, Eqs. (4) and (5) set the upper and lower bounds permitted for the *state* and *flow* variables. While the *state_min* and *state_cap* parameters were set for all temperature nodes for computational reasons, only the bounds shown in Table 1 were tight enough to impact model operation. Similarly, the heating and cooling units had their *capacity* parameters set according to the previous sections, sized to survive the baseline full-year simulations without issues. The PV generation was implemented using stochastic time series data for the *capacity* parameter, allowing the PV to be curtailed.

Four full-year simulations were performed in order to compare their performance:

Baseline was calculated directly from the input data without SpineOpt, assuming the district does not consider the hourly electricity prices. This meant the heating and cooling systems were simply operated to satisfy demand and thermal comfort, and the battery was charged and discharged solely to reduce electricity export and import for each hourly time step separately.

Perfect MPC only used the *Realization* scenario, thus having perfect information about the future.

Deterministic MPC used the *Mean* scenario, thus making decisions based solely on the expected future.

Stochastic MPC used the *Mean*, *Optimistic*, and *Pessimistic* scenarios with equal weights, giving the MPC an idea of the range of possible futures.

Note that the first hour of every window of all MPCs used the *Realization* scenario before branching into the forecast scenarios for the remaining 47 future hours, in order to simulate the MPC making decisions in real time. The full-year MPC simulations were performed using a rolling horizon approach, where the optimisation problem in Eqs. (1)–(5) was solved hourly, recording the resulting variable values only for the first *Realization* hour of each iteration.

Results

The full-year simulations were performed on a 64-bit Windows 10 laptop with a *Intel(R) Core(TM) i7-8665U CPU @ 1.90GHz 2.11 GHz* processor and 16 GB of RAM. The *Perfect* and *Deterministic MPCs* took roughly 2–3 hours to solve for the full year, while the *Stochastic MPC* took around 5–6 hours. This equals less than three seconds per solve, making real-time operation feasible. Figure 3 presents an illustration of the *Stochastic MPC* operation compared to the *Baseline* for example 48-hour periods during both winter and summer. Furthermore, Table 2 provides a summary of the key results of the simulated MPCs compared to the *Baseline*. Note that the presented costs were post-processed based on the final realised electricity consumption and prices for all MPCs, not on the expected future costs of each iteration represented by the objective function in Eq. (1).

The *Stochastic MPC* can be seen to perform as expected in Figure 3, saving costs in winter by shifting heating and cooling demand towards cheaper hours, as well as using the battery in a similar manner. This can also be seen in Table 2, with the total and average import costs reducing by 4.43–6.10 % and 15.81–16.18 % respectively despite the 11.92–13.53 % increase in total electricity imports across the different MPCs. While shifting the heating and cooling demand did result in increased electricity consumption between 2.81–4.66 % due to increased heat losses, it's

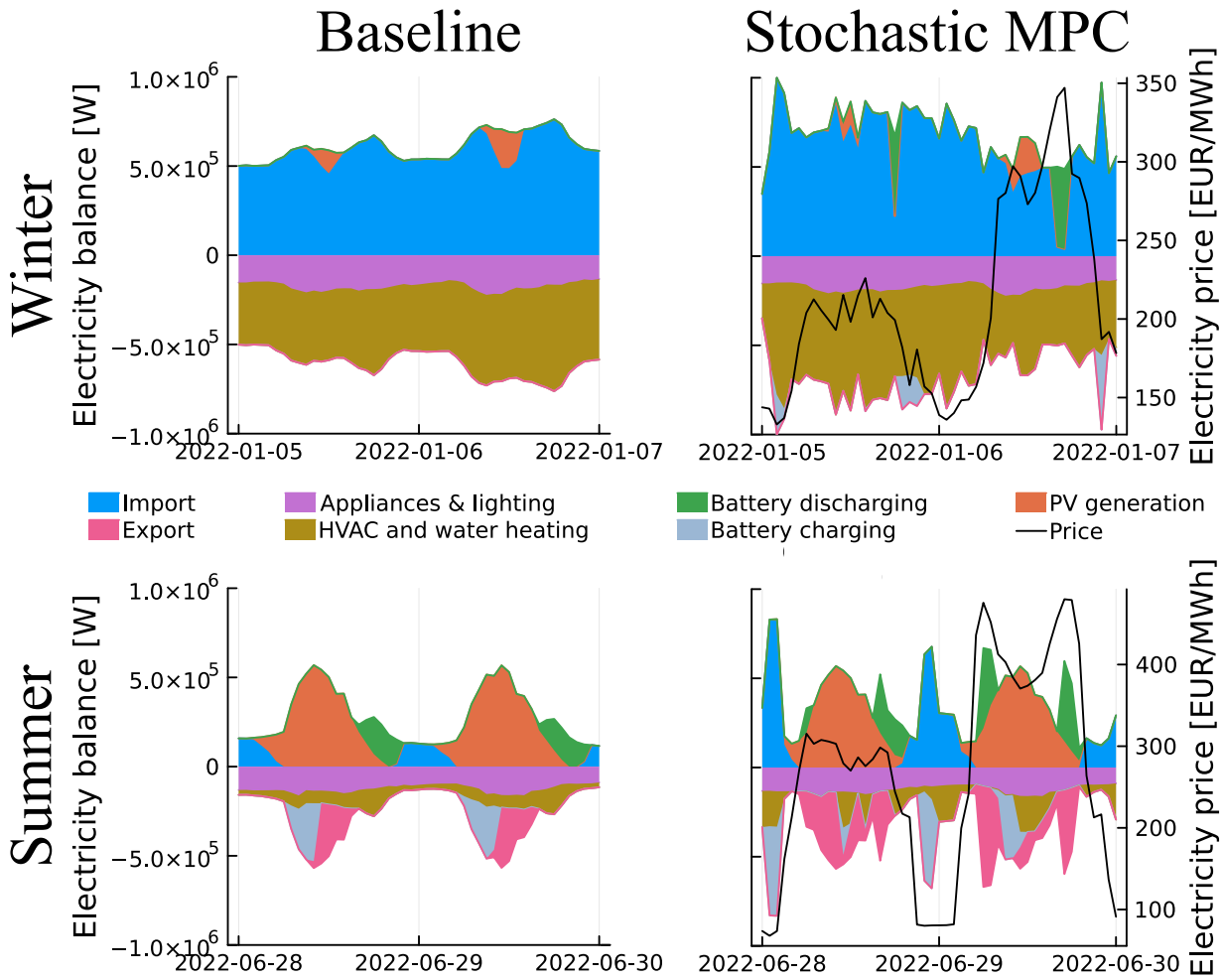

Figure 3: Baseline and Stochastic MPC district operation for example 48-hour periods. Electricity supply into the district is indicated by positive values, while electricity consumption is indicated by negative values. Furthermore, the areas above and below zero mirror each other, as the supply and demand of electricity within the district need to be in balance each hour.

Table 2: Summary of the key results and their change relative to the Baseline for each MPC.

Import & Export	Baseline	Perfect	Deterministic	Stochastic
Total import [MWh]	2340.33	2619.36 (11.92 %)	2625.22 (12.17 %)	2656.73 (13.52 %)
Total import costs [kEUR]	499.73	469.24 (-6.10 %)	469.86 (-5.98 %)	477.61 (-4.43 %)
Average import price [c/kWh]	21.35	17.91 (-16.10 %)	17.9 (-16.18 %)	17.98 (-15.81 %)
Total export [MWh]	146.54	320.94 (119.01 %)	321.13 (119.14 %)	319.56 (118.07 %)
Total export revenue [kEUR]	27.47	92.64 (237.27 %)	92.34 (236.17 %)	91.94 (234.70 %)
Average export price [c/kWh]	18.74	28.87 (54.00 %)	28.75 (53.40 %)	28.77 (53.48 %)
Total net costs [kEUR]	472.26	376.6 (-20.26 %)	377.52 (-20.06 %)	385.67 (-18.34 %)
Consumption & Generation				
Total heating electricity [MWh]	2177.23	2238.51 (2.81 %)	2244.41 (3.09 %)	2278.72 (4.66 %)
Total other electricity [MWh]	968.55	968.55 (0.00 %)	968.55 (0.00 %)	968.55 (0.00 %)
Total PV generation [MWh]	968.58	968.58 (0.00 %)	968.58 (0.00 %)	968.58 (0.00 %)
Total battery charging [MWh]	164.98	561.03 (240.06 %)	558.37 (238.45 %)	545.64 (230.74 %)
Total battery discharging [MWh]	148.39	503.97 (239.63 %)	501.56 (238.01 %)	490.07 (230.27 %)

not enough to account for the increased imports considering the MPCs had no control over other electric loads. Instead, the majority of the increased electricity imports were due to electricity trading with the battery in summer, seen to discharge during expensive hours in Figure 3. Table 2 also shows significant increases in battery charging and discharging by 230.27–240.06 %, exported electricity and its revenue by 118.07–119.14 % and 234.70–237.27 % respectively, as well as average export prices increasing by 53.40–54.00 %. Note that this behaviour is extremely dependent on the assumed electricity prices, though, and more conservative electricity price assumptions would likely result in more focus on increasing self-consumption.

The behaviour of the *Perfect*, *Deterministic*, and *Stochastic MPC* were very similar overall, with only slight deviations here and there accounting for the differences in Table 2. As expected, the *Perfect MPC* achieved the largest reduction in total net costs of 20.26 % compared to the *Baseline*, while the *Deterministic* and *Stochastic MPCs* achieved relative savings of 20.06 % and 18.34 % respectively. While the *Stochastic MPC* had more information about the range of possible futures than the *Deterministic MPC*, it does not necessarily translate to better performance. In this case, knowledge of the rather extreme *Optimistic* and *Pessimistic* forecasts resulted in the *Stochastic MPC* preferring more robust control, losing to the *Deterministic MPC* in terms of savings. However, it is entirely possible that tweaking the weights of the scenarios for the *Stochastic MPC* could result in it outperforming the *Deterministic MPC*, but such analysis is outside the scope of this work.

Overall, it is quite surprising how little difference there was between the *Deterministic* and *Stochastic MPCs* compared to the *Perfect MPC*. This would seem to indicate that the weather and load forecasts were of less importance to the MPC than the electricity prices, which were assumed to be known 12–36 hours in advance regardless of the MPC according to current NordPool day-ahead market clearing conventions. One possible explanation is, that only the space heating and cooling flexibility is directly influenced by weather conditions, while the battery is only indirectly affected through PV generation and load forecasts. Furthermore, due to lacking DHW demand profile data, the DHW storage tanks were practically independent of any forecasts, except for the electricity prices. Recent research by Rasku et al. (2023) also indicates that water heating offers more relative flexibility than space heating due to less dependence on ambient weather conditions.

Conclusions

This work demonstrates that SpineOpt is a viable tool for modelling district-level energy systems using a small imaginary six-building system with PV generation and a shared battery. Three economic MPCs using different 48-hour forecasts of future weather conditions, electric load, and electricity prices were implemented in SpineOpt, and solved hourly for the full year of 2022. Overall, the MPCs behaved as expected of their cost minimisation objective, achieving total net cost savings around 18.34–20.26 % in line with comparable existing literature reviewed by Taheri et al. (2022). Thus, a similar approach seems viable to be employed on city or nation-scale as well, depicting flexible building stock operation within large-scale energy system models. This, in turn, can help better capture the potential value of building-level flexibility in system-scale scenario analysis for the coming decades.

The performance of the *Perfect*, *Deterministic* and *Stochastic MPCs* was surprisingly similar, emphasising the importance of day-ahead electricity prices known in advance. Furthermore, the rather extreme electricity prices in 2022 seemed to encourage primarily utilising the common battery for exploiting the electricity price arbitrage in the summer, resulting in increased import and export volumes. While this is extremely dependent on the electricity import and export price assumptions, it does highlight the potential need for better electricity market bidding tools also on the district level. However, suitable business models and legislation are still required in order to make building energy flexibility attractive to the stakeholders.

Acknowledgements

This research was funded by the Academy of Finland project *Integration of building flexibility into future energy systems (FlexiB)* under grant agreement No 332421.

References

Arteconi, A., D. Patteeuw, K. Bruninx, E. Delarue, W. D'haeseleer, and L. Helsen (2016). Active demand response with electric heating systems: Impact of market penetration. *Applied Energy 177*, 636–648.

Bloess, A., W.-P. Schill, and A. Zerrahn (2018). Power-to-heat for renewable energy integration: A review of technologies, modeling approaches, and flexibility potentials. *Applied Energy 212*, 1611–1626.

Cooper, S. J. G., G. P. Hammond, M. C. McManus, and D. Pudjianto (2016). Detailed simulation of electrical demands due to nationwide adoption of heat pumps, taking account of renewable generation and mitigation. *IET Renewable Power Generation 10*(3), 380–387.

Drgoňa, J., J. Arroyo, I. Cupeiro Figueroa, D. Blum, K. Arendt, D. Kim, E. P. Ollé, J. Oravec, M. Wetter, D. L. Vrabie, and L. Helsen (2020). All you need to know about model predictive control for buildings. *Annual Reviews in Control 50*, 190–232.

EQUA Simulation AB and Aalto University (2013). IDA Early Stage Building Optimization (ESBO) v1.13.

Eskola, L., J. Jokisalo, and K. Sirén (2012). Lämpöpumppujen energialaskentaopas (energy calculation guide for heat pumps). In Finnish.

Finnish Ministry of the Environment (2017). Ympäristöministeriön asetus uuden rakennuksen sisäilmastosta ja ilmanvaihdosta (Ministry of the Environment statute on the indoor climate and ventilation of new buildings).

Godahewa, R., C. Bergmeir, G. Webb, R. Hyndman, and P. Montero-Manso (2020). Electricity hourly dataset. Obtained from Zenodo: https://doi.org/10.5281/zenodo.4656140.

Hedegaard, K. and O. Balyk (2013). Energy system investment model incorporating heat pumps with thermal storage in buildings and buffer tanks. *Energy 63*, 356–365.

Hersbach, H., B. Bell, P. Berrisford, S. Hirahara, A. Horányi, J. Muñoz-Sabater, J. Nicolas, C. Peubey, R. Radu, D. Schepers, A. Simmons, C. Soci, S. Abdalla, X. Abellan, G. Balsamo, P. Bechtold, G. Biavati, J. Bidlot, M. Bonavita, G. De Chiara, P. Dahlgren, D. Dee, M. Diamantakis, R. Dragani, J. Flemming, R. Forbes, M. Fuentes, A. Geer, L. Haimberger, S. Healy, R. J. Hogan, E. Hólm, M. Janisková, S. Keeley, P. Laloyaux, P. Lopez, C. Lupu, G. Radnoti, P. de Rosnay, I. Rozum, F. Vamborg, S. Villaume, and J.-N. Thépaut (2020). The ERA5 global reanalysis. *Quarterly Journal of the Royal Meteorological Society 146*(730), 1999–2049.

Hofmann, F., J. Hampp, F. Neumann, T. Brown, and J. Hörsch (2021). atlite: A lightweight python package for calculating renewable power potentials and time series. *Journal of Open Source Software 6*(62), 3294.

Huckebrink, D. and V. Bertsch (2022). Decarbonising the residential heating sector: A techno-economic assessment of selected technologies. *Energy 257*, 124605.

Ihlemann, M., I. Kouveliotis-Lysikatos, J. Huang, J. Dillon, C. O'Dwyer, T. Rasku, M. Marin, K. Poncelet, and J. Kiviluoma (2022). SpineOpt: A flexible open-source energy system modelling framework. *Energy Strategy Reviews 43*, 100902.

Kiviluoma, J., F. Pallonetto, M. Marin, P. T. Savolainen, A. Soininen, P. Vennström, E. Rinne, J. Huang, I. Kouveliotis-Lysikatos, M. Ihlemann, E. Delarue, C. O'Dwyer, T. O'Donnel, M. Amelin, L. Söder, and J. Dillon (2022). Spine toolbox: A flexible open-source workflow management system with scenario and data management. *SoftwareX 17*, 100967.

Kurnitski, J., P. Kalliomäki, M. Haakana, J. Shemeikka, A. Laitininen, K. Krzysztof, M. Saari, and P. Kukkonen (2011). Lämmitysjärjestelmät ja lämmin käyttövesi - laskentaopas (heating systems and domestic hot water - calculation guide). In Finnish.

Rasku, T. (2022). ArchetypeBuildingModel.jl. Zenodo. https://doi.org/10.5281/zenodo.7729342.

Rasku, T. (2023). FlexiB Spine Toolbox workflow for BS2023 stochastic MPC using SpineOpt. Zenodo. https://doi.org/10.5281/zenodo.7733559.

Rasku, T. and J. Kiviluoma (2018). A comparison of widespread flexible residential electric heating and energy efficiency in a future nordic power system. *Energies 12*(1), 5.

Rasku, T., T. Lastusilta, A. Hasan, R. Ramesh, and J. Kiviluoma (2023). Economic model-predictive control of building heating systems using Backbone energy system modelling framework. Preprint. Zenodo. https://doi.org/10.5281/zenodo.7767364.

Rasku, T., R. Simson, and J. Kiviluoma (2023). Sensitivity of a simple lumped-capacitance building thermal modelling approach intended for building-stock-scale flexibility studies. Preprint. Zenodo. https://doi.org/10.5281/zenodo.7623740.

Taheri, S., P. Hosseini, and A. Razban (2022). Model predictive control of heating, ventilation, and air conditioning (hvac) systems: A state-of-the-art review. *Journal of Building Engineering 60*, 105067.